Pis'ma v ZhETF, vol. 96, iss. 4, pp. 247 – 251

ODMR of Mn-related excitations in (Cd,Mn)Te quantum wells

D. O. Tolmachev[1)], *A. S. Gurin, N. G. Romanov, A. G. Badalyan, R. A. Babunts, P. G. Baranov, B. R. Namozov, Y. G. Kusrayev*

Ioffe Physical-Technical Institute, 194021 St.-Petersburg, Russia

Submitted 3 July 2012

Optically detected magnetic resonance (ODMR) was applied to reveal the exchange interaction effects between Mn^{2+} ions and confined holes in (Cd,Mn)Te quantum wells with 2D hole gas. Two anisotropic ODMR signals with different angular variations were found and ascribed to isolated manganese ions and to exchange-coupled complexes consisting of manganese and holes. It is shown that calculations on the basis of spin Hamiltonian for these systems are in agreement with the experimental data.

1. Introduction. Diluted magnetic semiconductors (DMS) are of considerable interest due to the possibility of applications combining electronic and spin effects – spintronics. Over the past ten years or so, the field of ferromagnetism in DMS has developed into an important branch of materials science [1]. The comprehensive research on these systems has been stimulated by a succession of demonstrations of outstanding low-temperature functionalities in (Ga,Mn)As, *p*-(Cd,Mn)Te and related structures. DMS are attractive objects to study the interaction of localized magnetic moments through indirect exchange coupling mediated by free carriers. The strong interactions between the two spin subsystems – free electrons or holes and localized transition element impurity spins give rise to the giant Zeeman splitting [2] of both the conduction and valence bands.

The manganese acceptors are known to behave unusually in some semiconductors, e.g., the electronic ground state of the neutral manganese acceptor in GaAs was shown in Ref. [3, 4] to be formed by a delocalized hole weakly coupled to the A- ($3d^5$) acceptor core, that is manganese which is anomalous member of the $3d$-transition metal family in compound semiconductors.

Electron paramagnetic resonance (EPR) is a method of choice for the study of transition metal ions [5]. The traditional methods of radiospectroscopy are hardly applicable for low-dimensional systems because of a decreased active volume and not high enough sensitivity, and because of the difficulty of separating contributions from the structure itself and the substrate. This difficulty can be overcome by employing optically detected magnetic resonance (ODMR). ODMR is now well established as a powerful tool in the semiconductor and solid-state physics which allows identification of the luminescence and optical absorption features and provides detailed information about the electronic structure of the defects and excitons (see, for example, refs. in [6]). High sensitivity, extreme resolution and spatial selectivity of ODMR make this technique very suitable for a study of quantum wells (QWs), superlattices (SLs), quantum dots (QDs) and nanocrystals [7].

ODMR was applied to several Mn doped II–VI compounds (see [8] and references therein). ODMR in single CdMnTe QW was studied in [9]. However, no anisotropy of the ODMR spectra was reported until our recent publications [10, 11], where anisotropic behavior of the center of gravity of the ODMR spectrum in CdMnSe/ZnSe quantum dots and CdMnSe/ZnSe submonolayer quantum wells has been observed. It was explained by the fine structure splitting of Mn^{2+}, which was ascribed to low dimensionality.

In spin-flip Raman-scattering studies of CdMnTe QWs containing a two-dimentional hole gas (2DHG) interacting with magnetic ions a reduction in the effective Mn g-factor with increasing hole concentration was found [12], which is predicted to occur prior to the ferromagnetic phase transition. The purpose of the present paper is to report the results of application of ODMR spectroscopy for a study of these QWs.

2. Experimental. Single 100 Å $Cd_{1-x}Mn_xTe$ QWs (x = 1, 2, 4%) were grown by molecular-beam epitaxy on (001)-oriented GaAs substrates with thick CdTe buffers and $Cd_{0.8}Mg_{0.2}Te$ barriers. The QWs were covered by thin $Cd_{0.8}Mg_{0.2}Te$ cap layers. A scheme of the structure under study is shown in top of Fig. 1. Though these QWs are not specially doped, owing to the surface states they contain a 2DHG. We studied QWs with a cap layer thickness of 17 nm, where the surface-state induced p-type doping is most effective [12]. For comparison similar CdMnTe QW without 2D hole gas were also studied.

35 and 94 GHz ODMR was recorded at 1.8 K via photoluminescence (PL) of excitons in QWs either using on-off modulation of microwaves and lock-in ampli-

[1)] e-mail: Daniel.Tolmachev@gmail.com

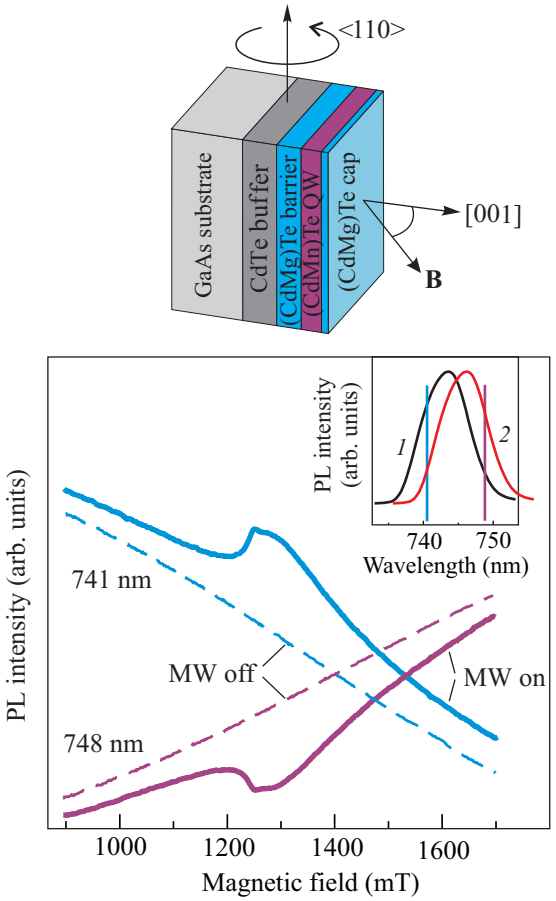

Fig. 1. The scheme of the QW structure under study (top), luminescence spectra of a 10 nm CdMnTe/CdMgTe QW (2% of Mn, the cap layer 17 nm) measured with wide slits at magnetic fields of 900 (*1*) and 1700 (*2*) mT (insert), and the magnetic field dependences of the emission intensity measured with microwaves on (solid lines) and off (dashed lines) at the wavelengths marked by vertical lines in the insert. $\nu = 35$ GHz, $P = 300$ mW. The angle θ between the magnetic field and the [001] growth axis of the QW is 60°

fication or without modulation of microwaves. Photoluminescence was excited with a 650 nm semiconductor laser and detected with a grating monochromator and a PM tube. In 35 GHz ODMR spectrometer the sample was placed in the centre of a cylindrical microwave cavity with holes for excitation and detection of PL. For 94 GHz ODMR a quasi-optical microwave system was used, which consisted from a horn antenna, a Teflon lens, and another horn antenna inserted in the cryostat. Microwave generators provided up to 1 W in 35 GHz and 100 mW at 94 GHz. The sample was mounted on a rotating sample holder, which enabled rotation of the sample in magnetic field.

3. Results and discussion. The PL spectra of the 10 nm $Cd_{0.98}Mn_{0.02}Te$/CdMgTe QWs with 2DHG consist from the emission lines of excitons and negatively charged excitons which shift to longer wavelengths with increasing magnetic field [12]. For ODMR measurements we used wide slits of the monochromator, which resulted in a broadening of the PL spectrum and made it possible to monitor the shift of the PL lines by measuring the emission intensity at a fixed wavelength. The PL spectrum (insert) and the magnetic field dependencies of the PL intensity at the wavelengths marked by vertical lines are shown in Fig. 1. The PL spectra were measured at a temperature of 1.8 K and magnetic field of 900 (*1*) and 1700 (*2*) mT with 35 GHz microwaves on. Solid and dashed lines show the magnetic field dependencies of the emission intensity measured with microwaves on and microwaves off, respectively. The angle θ between the magnetic field and the [001] growth axis of the QW is 60°.

One can see that without microwaves the dependencies of the PL intensity on the magnetic field in the range 900–1700 mT are close to linear, which corresponds to a practically linear shift of the PL line to longer wavelengths with the increasing field. Application of the 35 GHz microwaves results in two effects: i) a parallel shift of the curves that is due to a microwave-induced non-resonant heating and ii) appearance of magnetic resonance lines.

Fig. 2 presents the angular variations of the ODMR spectra measured at $T = 1.8$ K and the microwave frequency of 35.1 (a) and 94.0 (b) GHz as the microwave-induced variations of the PL intensity for different orientations of the magnetic field relative to the [001] growth direction in the (110) plane. The ODMR signals can be decomposed into two anisotropic components, i.e., a broad line which shifts to higher fields with increasing θ and a narrower line which manifests a slight shift in opposite direction, i.e., to lower fields. The results of decomposition of the ODMR spectra into two lines are shown below the experimental curves.

To clarify the origin of the observed ODMR spectra we have studied a similar structure which did not contain 2DHG. Fig. 3 shows the angular variations of the ODMR spectra of 12 nm $Cd_{0.98}Mn_{0.02}Te$/CdMgTe QW measured at the microwave frequencies of 35.1 (a) and 94 (b) GHz. The ODMR spectra manifest the same behavior as the narrow line in Fig. 2, i.e. a slight shift to lower fields with increasing θ. For comparison these ODMR signals are plotted in Fig. 2 below the simulated ODMR spectra.

The observed ODMR spectra are definitely connected with Mn^{2+} ions. The g-factor of individual Mn^{2+} ions is known to be isotropic and close to $g = 2$, and therefore cannot give rise to an anisotropy of the ODMR

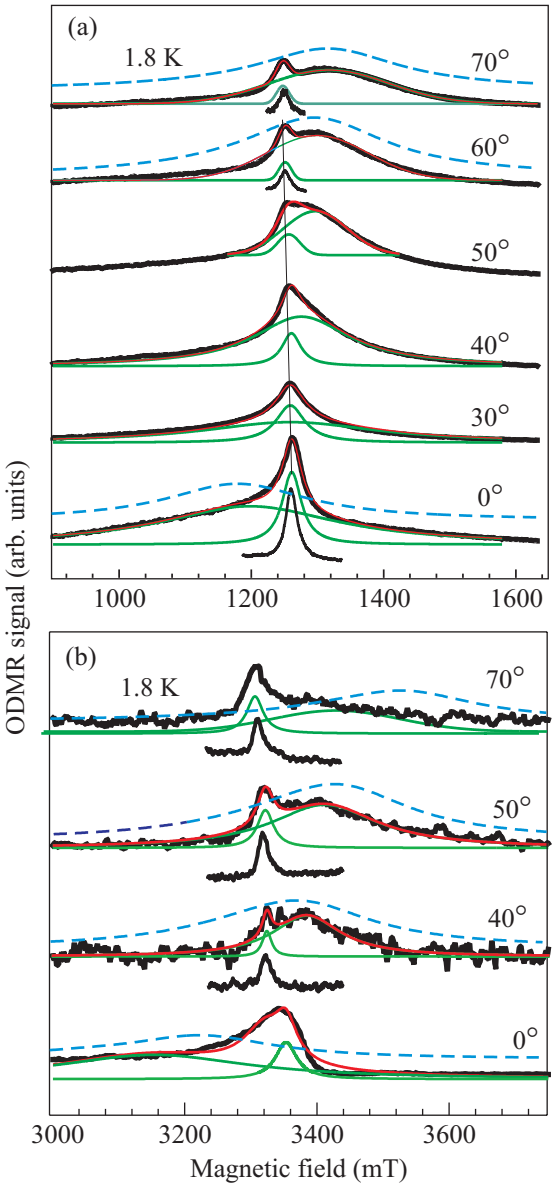

Fig. 2. ODMR spectra of 10 nm CdMnTe/CdMgTe QW (2% of Mn, the cap layer 17 nm) measured at the microwave frequencies of 35.1 (a) and 94 (b) GHz for different orientations of the magnetic field relative to the [001] growth axis. The results of decomposition of the ODMR spectra into two lines are shown below the experimental curves. The dashed lines show the results of theoretical simulation using the spin Hamiltonian (2, 3). For simulation a Lorentzian line with a width of 150 mT was used to account for a spread of the exchange interactions. The ODMR spectra recorded in 12 nm CdMnTe/CdMgTe QW (2% of Mn) without 2DHG are shown for some orientations below the simulated spectra.

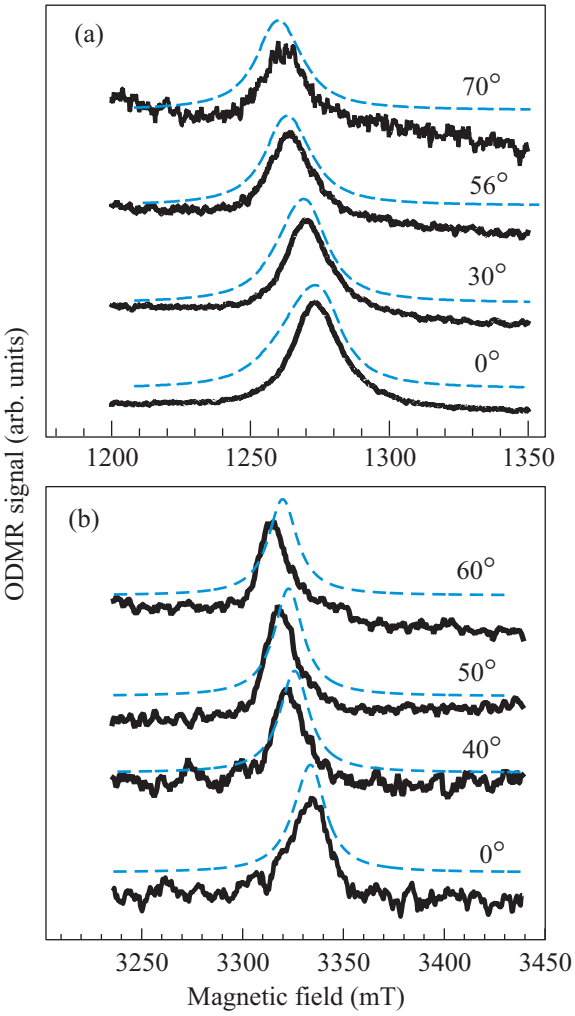

Fig. 3. Angular variations of the ODMR spectra of 12 nm CdMnTe/CdMgTe QW (2% of Mn) measured at T = = 1.8 K and the microwave frequencies of 35.1 (a) and 94 (b) GHz. The dashed lines show the results of theoretical simulation using the spin Hamiltonian (1) with $D = 30 \cdot 10^{-4}$ cm^{-1}. For simulation a Lorentzian line with a width of 10 mT was used to account for a spread of the D values

signal. In Ref. [10] the anisotropy of the Mn^{2+} ODMR spectra in CdMnSe QDs was ascribed to the axial ([001]) fine structure with a strong positive zero-field splitting. The anisotropy of the center of gravity of the ODMR spectra, which are envelopes of the fine and hyperfine structure lines, appears because of the large Boltzmann factor characteristic of high magnetic fields and low temperatures. An example of anisotropic behavior of the EPR spectra of Mn^{2+}, which is connected with different intensities of the fine structure transitions, was given in Ref. [10] for Mn^{2+} in ZnO.

ODMR spectra for isolated Mn^{2+} can be described with the spin Hamiltonian

$$\hat{H}_{Mn} = g\mu_B \mathbf{B} \cdot \mathbf{S} + D\left[S_Z^2 - \frac{1}{3}S(S+1)\right], \qquad (1)$$

where μ_B is Bohr magneton, $g = 2.0032$ and is isotropic, $S = 5/2$, and D is a zero-field splitting parameter for the axial crystal field. At thermal equilibrium the lowest fine-structure levels of Mn^{2+} are more populated and the $M_S = -5/2 \leftrightarrow M_S = -3/2$ and $M_S = -3/2 \leftrightarrow M_S = -1/2$ EPR transitions dominate the spectra. This results in angular variation of the observed ODMR signals. The symmetry of the fine-structure splitting, which is due to the crystal field, is consistent with the [001] growth direction.

The estimated value of the zero-field splitting in 12 nm CdMnTe QW under study $D = 30 \cdot 10^{-4}$ cm^{-1} is much smaller than that obtained for CdMnSe QDs ($D = 200 \cdot 10^{-4}$ cm^{-1}) investigated in Ref. [10] and is close to the value obtained for CdMnSe QWs [11]. The hyperfine structure of Mn is not resolved in the ODMR spectra most probably because of a distribution of the D values and a difference in the effect of different fine structure levels on the PL shift. The dashed lines in Fig. 3 show the results of simulation of the ODMR spectra using the spin Hamiltonian (1) with $D = 30 \cdot 10^{-4}$ cm^{-1} and taking into account the Boltzmann distribution of populations for the fine structure levels. For simulation Lorentzian line shape and a line width of 10 mT were used to account for a spread of the D values. Thus, the narrow line in $Cd_{0.98}Mn_{0.02}Te$/CdMgTe QWs with 2D hole gas can be considered as a fingerprint of isolated Mn^{2+} ions.

A similar behavior of the ODMR spectra has been observed at 94 GHz. It is to be noted that the shift of the ODMR lines is a little larger for the 94 GHz ODMR spectra than for the 35 GHz ODMR but is far from being proportional to the microwave frequency. This shows unambiguously that the shift is not determined by a g-factor shift.

As was mentioned above in QWs containing 2D hole gas, a strongly anisotropic wide ODMR line is observed in addition to a usual ODMR signal of Mn. The effective g-factor of this wide line varies from $g \approx 2.07$ at $\theta = 0^\circ$ to $g \approx 1.86$ at $\theta = 70^\circ$. We tentatively ascribe this line to exchange-coupled complexes consisting of the manganese and the holes.

The energy levels of a pair which is formed by Mn^{2+} and holes in a CdMnTe QW can be described by the Hamiltonian

$$\hat{H}_{\text{exc}} = \hat{H}_{\text{Mn}} + \hat{H}_h + \mathbf{J}_h \hat{c} \mathbf{S}_{\text{Mn}}, \qquad (2)$$

where the first two terms describe the Zeeman interactions for Mn^{2+} with $S = 5/2$ and a hole with the momentum J_h and the third term is their exchange interaction. $\hat{H}_{\text{Mn}}$ is given by Eq. (1).

In zinc blende semiconductors, such as CdTe, the valence band is split by spin-orbit coupling into a lower band ($J = 1/2$) and an upper band ($J = 3/2$) which is fourfold degenerate at the Brillouin zone center Γ. Thus, the top of the valence band consists of the heavy- and light-hole subbands, each twofold degenerate in angular-momentum projection. The heavy-hole subband states are characterized by the angular momentum projections of $\pm 3/2$, and the light-hole subband states, by $\pm 1/2$. An axial strain usually present in quantum-well structures, results in a partial lifting of valence band degeneracy. The upper band is further split into two components with $J_z = \pm 3/2$ (heavy hole) and $J_z \pm 1/2$ (light hole), separated by more than 10 meV. At liquid-helium temperature only the heavy-hole energy levels $J_z = \pm 3/2$ are populated. For the magnetic fields used in the ODMR experiments the Zeeman energy splittings are much smaller than the difference in confinement energy for the light and heavy holes. This means that we can describe the magnetic properties of the light- and heavy holes separately.

The heavy hole states can be described with the effective spin $S^* = 1/2$:

$$\hat{H}_h = \mu_B [g_{h\parallel} B_z S_z^* + g_{h\perp} (B_x S_x^* + B_y S_y^*)], \qquad (3)$$

where $g_\parallel$ and $g_\perp$ are the components of the $\hat{g}$ tensor along the [001] growth axis (z-axis) and perpendicular to it. According to a theoretical consideration the heavy hole spin is frozen in the growth direction due to quantum confinement or, equivalently, its in-plane g factor is vanishing. This implies that the in-plane magnetization equals to zero. In an ideal QW having D_{2d} symmetry, only the longitudinal component of the heavy-hole g factor tensor g_{zz} is appreciable. Thus, the spin Hamiltonian for an exchange-coupled pair of Mn and a hole can be rewritten as:

$$\hat{H}_{\text{exc}} = \hat{H}_{\text{Mn}} + \hat{H}_h + c\hat{S}^* \hat{S}_{\text{Mn}}, \qquad (4)$$

where c is the isotropic exchange interaction constant. As a result of the exchange interaction the total spin of the system can be written as the sum of the spin of Mn^{2+} ion and the hole effective spin: $\hat{S}_{\text{Mn}} + \hat{S}^*$, which leads to $S = 3$ and 2. For the ferromagnetic interaction coefficient c is negative and the level of $S = 3$ state has the lowest energy. The energy levels for such a system are shown on Fig. 4.

This is of cause a rough approximation. Here we consider the interaction of a Mn^{2+} ion with a single hole. Calculations have shown, however that the results were not changed considerably for the case of the exchange interaction of Mn^{2+} with two, three, and four holes simultaneously. In this calculations the last term in (4)

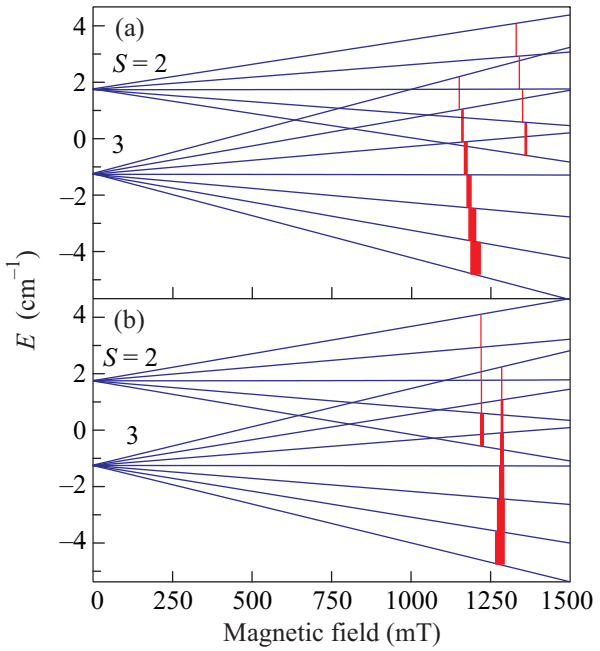

Fig. 4. Energy levels of an exchange-coupled pair Mn^{2+} – confined hole ($c = -1\,\mathrm{cm}^{-1}$) calculated for $\theta = 0°$ (a) and 70° (b). The thickness of vertical lines which mark the 35 GHz EPR transitions reflects symbolically the Boltzmann distribution of the level populations

should be replaced by the sum $\hat{S}_{\mathrm{Mn}} \cdot \sum c_i \hat{S}_i^*$, where $\hat{S}_i^*$ and c_i are the effective spin and the exchange interaction for hole number i.

The dashed lines in Fig. 2 show the results of theoretical simulation of ODMR spectra with the spin Hamiltonians (2)–(4). The large Boltzmann factor leading to the preferential occupancy of the lowest energy sublevels was taken into consideration. For simulation the 150 mT Lorentzian line was used to account for a spread of the exchange interactions. The simulation was done with the following parameters: the hole g-factors $g_{zh} = 2.8$ and $g_{xh} = g_{yh} = g_{\perp h} = 1$, $c = -1\ \mathrm{cm}^{-1}$.

In summary, two anisotropic ODMR signals with different angular variations were found and ascribed to isolated manganese ions and to exchange-coupled complexes consisting of manganese and confined holes in (Cd,Mn)Te quantum wells with 2D hole gas. The calculations on the basis of spin Hamiltonian for these systems were shown to be in agreement with the experimental data.

This work has been supported by Ministry of Education and Science, Russia, under the Contract # 16.513.12.3007; the Programs of the Russian Academy of Sciences "Spin Phenomena in Solid State Nanostructures and Spintronics", "Fundamentals of Nanostructure and Nanomaterial Technologies" and by the Russian Foundation for Basic Research under Grant # 12-02-01011.

1. T. Dietl, Nature materials **9**, 965 (2010) and references therin.
2. A. V. Komarov, S. M. Ryabchenko, O. V. Terletskii, et al., Sov. Phys. JETP **46**, 318 (1977).
3. J. Schneider, U. Kaufmann, W. Wilkening et al., Phys. Rev. Lett. **59**, 240 (1987).
4. V. F. Masterov, S. B. Mikhrin, B. E. Samorukov et al., Fiz. Tekh. Poluprovodn. **17**, 1259 (1983) [Sov. Phys. Semicond. **17**, 796 (1983)].
5. A. Abragam and B. Bleaney, *Electron Paramagnetic Resonance of Transition Ions*, Oxford University Press, Oxford, 1970.
6. B. C. Cavenett, Adv. Phys. **4**, 475 (1981).
7. P. G. Baranov and N. G. Romanov, Appl. Magn. Resonance **21**, 165 (2001).
8. V. Yu. Ivanov and M. Godlewski, Appl. Magn. Reson. **39**, 31 (2010).
9. M. L. Sadowski, M. Byszewski, M. Potemski et al., Appl. Phys. Lett. **82**, 3719 (2003).
10. P. G. Baranov, N. G. Romanov, D. O. Tolmachev et al., JETP Lett. **88**, 631 (2008).
11. D. O. Tolmachev, R. A. Babunts, N. G. Romanov et al., Phys. Status Solidi B **247**, 1511 (2010).
12. C. Kehl, G. V. Astakhov, K. V. Kavokin et al., Phys. Rev. B **80**, 241203 (2009).